

CHROM. 11,665

## EVALUATION OF THE CHARACTERISTICS OF THE DIFFERENTIAL AMPEROMETRIC DETECTOR IN COMBINATION WITH ANION-EXCHANGE CHROMATOGRAPHY, USING L-ASCORBIC ACID AS TEST COMPOUND

K. BRUNT and C. H. P. BRUINS

*Laboratory of Pharmaceutical and Analytical Chemistry, State University, Antonius Deusinglaan 2, 9713 AW Groningen (The Netherlands)*

(First received October 24th, 1978; revised manuscript received December 13th, 1978)

---

### SUMMARY

The hydrodynamic characteristics of the thin-layer flow cell of the differential amperometric detector were deduced theoretically and confirmed by experiment. The response of the differential amperometric detector was compared with that of a fixed-wavelength UV detector in the analysis of L-ascorbic acid in combination with anion-exchange chromatography.

---

### INTRODUCTION

Recently, we reported the use of the differential amperometric detector<sup>1</sup> in high-performance liquid chromatography (HPLC) and described the design of the thin-layer flow cell. A scheme for the pumping system in combination with the differential amperometric detector was discussed and typical response peaks of the detector for 5-ng samples of L-ascorbic acid in flow injection analysis were shown.

In this paper, we present more detailed information about the detector, compare the response with that of a UV detector and describe some applications of the differential amperometric detector in combination with ion-exchange chromatography.

#### *Design of the electronic circuits of the detector*

As can be seen in Fig. 1, the differential amperometric detector consists of a simple potentiostat, two current followers coupled by a differential amplifier, an offset circuit and an amplifier for the desired sensitivity of the output signal. The polarity and potential (0-2.5 V) of both working electrodes ( $W_1$  and  $W_2$ ) with respect to the saturated calomel reference electrode (ref) can be simply adjusted by switch  $S_1$  and trimmer  $R_2$ .

To protect the working electrodes from contamination, it is advisable to disconnect both working electrodes from the current followers  $A_2$  and  $A_3$  with switch  $S_2$  when no measurements are being made. With switch  $S_3$  and trimmer  $R_{11}$  it is possible

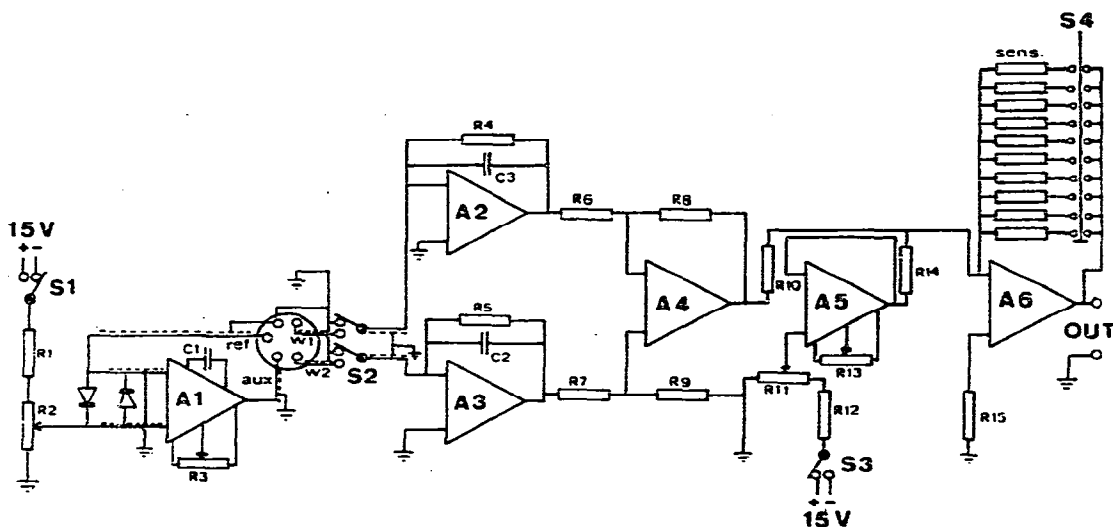


Fig. 1. Circuit diagram of the differential amperometric detector.  $R_1 = 30\text{ k}\Omega$ ;  $R_2 = 5\text{ k}\Omega$ ;  $R_3 = 100\text{ k}\Omega$ ;  $R_4 = 10\text{ M}\Omega$ ;  $R_5 = 10\text{ M}\Omega$ ;  $R_6 = 10\text{ k}\Omega$ ;  $R_7 = 10\text{ k}\Omega$ ;  $R_8 = 10\text{ k}\Omega$ ;  $R_9 = 10\text{ k}\Omega$ ;  $R_{10} = 4\text{ k } 99\Omega$ ;  $R_{11} = 5\text{ k}\Omega$ ;  $R_{12} = 30\text{ k}\Omega$ ;  $R_{13} = 10\text{ k}\Omega$ ;  $R_{14} = 4\text{ k } 99\Omega$ ;  $R_{15} = 2\text{ k } 15\Omega$ ;  $C_1 = 220\text{ pF}$ ;  $C_2 = 0.47\text{ }\mu\text{F}$ ;  $C_3 = 0.47\text{ }\mu\text{F}$ ;  $A_1 = \text{OP } 05$ ;  $A_2 = 0042$ ;  $A_3 = 0042$ ;  $A_4 = 0042$ ;  $A_5 = \mu\text{A } 741$ ;  $A_6 = 0042$ . Sensitivity,  $0.1\text{--}100\text{ nA/V}$ .  $R = 4\text{ k } 99\Omega\text{--}5\text{ M}\Omega$ .

to balance the signals of the reference cell and the measuring cell by means of an off-set circuit.

The desired current range of the output of the detector can be adjusted with switch  $S_4$ . All of the wires used for connecting the electrodes to the detector electronics are shielded.

For ease of understanding the electronic circuit, the off-set trimmers ( $10\text{ k}\Omega$ ) of the operational amplifiers  $A_2$ ,  $A_3$ ,  $A_4$  and  $A_5$  have been omitted.

#### *Hydrodynamics of the thin-layer flow cell*

The symbols used are defined at the end of the paper.

For the theoretical discussion the following assumptions are made: the cell is a rectangular flow channel; the fluid is newtonian; diffusion in the direction of flow is neglected; the reaction takes place at one plate of the cell; and boundary effects at the vertical walls of the thin layer cell are neglected.

The behaviour of the fluid flow in the detector cell can be described by hydrodynamics<sup>2,3</sup>. The usual criterion for the existence of a laminar flow is

$$Re = \frac{\bar{u}d}{\nu} < 2300 \quad (1)$$

Fluid often flows through channels of non-circular cross-section, and therefore it is convenient to define the hydraulic diameter,  $d_h$ :

$$d_h = \frac{4A}{B} \quad (2)$$

For a rectangular flow channel formed by two parallel planes, where the gap  $h$  is much smaller than the width  $b$ ,

$$d_h = \frac{4bh}{2(b+h)} \approx 2h \quad (3)$$

Considering the dimensions of the thin-layer cell and the flow-rates used in HPLC, the Reynolds number is small ( $Re = 7.2$  for a flow-rate of  $1.2 \text{ ml} \cdot \text{min}^{-1}$  and a spacer thickness of  $127 \mu\text{m}$ ), so the fluid flow in the cell is laminar. Therefore, the mass transport of the electroactive components from the bulk of the eluent in the thin-layer cell to the electrode surface occurs by diffusion. This indicates that the detector response is diffusion limited. Consider the case in which the reaction surface is a smooth plate with a fluid flowing laminar across it and that the length and width of the plate are significantly larger than the thickness of the hydrodynamic boundary layer. If we also assume that the reaction rate is infinitely large compared with the rate of mass transfer, we obtain a diffusional flow problem which has been described by Levich<sup>3</sup>. The thickness of the diffusion layer on the plate is

$$\delta \approx 3\left(\frac{D}{\nu}\right)^{\frac{1}{2}} \sqrt{\frac{\nu x}{U}} \quad (4)$$

The diffusional flux to the plate is given by

$$j = D\left(\frac{\partial c}{\partial y}\right)_{y=0} = 0.34 \frac{Dc_0\sqrt{U}}{\sqrt{\nu x}} \left(\frac{\nu}{D}\right)^{\frac{1}{2}} = \frac{Dc_0}{\delta} \quad (5)$$

The total diffusion flow to the surface of the plate can be obtained by integrating  $j_{\text{max}}$  along the surface:

$$I_{\text{max.}} = 0.68 Dc_0b \left(\frac{\nu}{D}\right)^{\frac{1}{2}} \sqrt{\frac{Ul}{\nu}} \quad (6)$$

The total diffusional flow,  $I_{\text{max.}}$ , is related by the factor  $nF$  to the electronic current through the electrode and is thus related to the detector output. Eqn. 6 indicates that  $I_{\text{max.}}$  depends on, among other factors, the dimensions of the electrode surface. Lankelma and Poppe<sup>4</sup> used this in their design of a coulometric flow cell by choosing a very large electrode surface. Once the dimensions of the electrode surface have been fixed, the detector response depends only on the concentration and the fluid velocity, assuming that  $\nu$  as a characteristic of the mobile phase and  $D$  as a characteristic of a sample in the mobile phase are constant. Although the reactive surface in our thin-layer cell is not a rectangular plate but consists of a circular plate countersunk in the wall of the cell, the dependence of the detector response on  $c_0$  and  $\sqrt{U}$  remains valid, as is shown under Results and Discussion.

## EXPERIMENTAL

### Apparatus

The HPLC high-pressure pumping system consisted of a Milton Roy Duplex

Mini Pump or a Spectra Physics 740 pump with pump control and pressure monitor (Type 3500B). An FMI laboratory pump (Model RP 154-55) pumped the mobile phase through the reference tubes and reference cell of the detector. The flow cell of the differential amperometric detector was made of Perspex and has been described elsewhere<sup>1</sup>. A Rheodyne valve (Model 70-10) with a 20- $\mu$ l sample loop was used as the sample injection system. The differential amperometric detector was compared with a Chromatronic UV absorbance detector (Model 220) with a fixed wavelength of 254 nm. Different columns were used of I.D. 2.1 or 4.6 mm and length 15–34 cm. The impedance measurements were made with a Radiometer Type CDM 2 conductivity meter.

### Chemicals

All of the chemicals were of analytical-reagent grade and were used without further purification. The mobile phase consisted of 0.1 M acetic acid adjusted to the desired pH with pellets of sodium hydroxide and was degassed by refluxing continuously. A strong anion-exchange resin (Nucleosil 10 SB) was used as the stationary phase.

## RESULTS AND DISCUSSION

### Effect of flow-rate on detector response

L-Ascorbic acid was used as the test compound. The linear fluid velocity,  $U$ , in eqn. 6 in the thin-layer cell corresponds to  $U_{\max}$  in the parabolic velocity distribution of a plane Poiseuille flow. According to basic hydrodynamics<sup>2</sup>,  $U_{\max} = \frac{3}{2} \bar{u}$  and is therefore directly related to the flow-rate of the mobile phase. Increasing the flow-rate

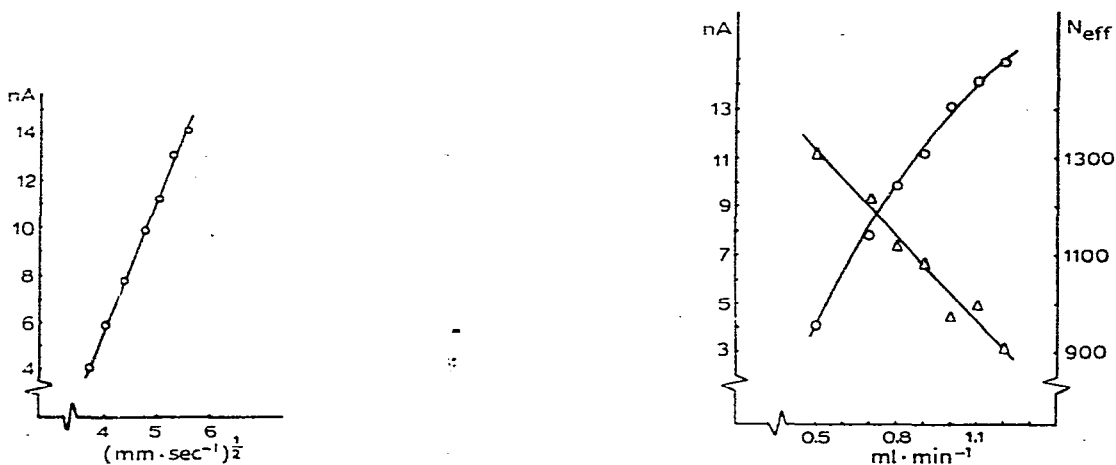


Fig. 2. Influence of  $\sqrt{\bar{u}}$  on peak height. Column, 150  $\times$  4.6 mm I.D. Nucleosil SB-10 anion exchanger. Eluent, 0.1 M acetic acid buffer (pH 4.5). Potential of working electrodes, 750 mV vs. S.C.E. Sample, 50 ng of L-ascorbic acid in 20  $\mu$ l. Spacer, 127  $\mu$ m.

Fig. 3. Influence of flow-rate on the effective plate number ( $\Delta$ ) and the peak height ( $\circ$ ). Column, 150  $\times$  4.6 mm I.D. Nucleosil SB-10 anion exchanger. Eluent, 0.1 M acetic acid buffer (pH 4.5). Potential of working electrodes, 750 mV vs. S.C.E. Sample, 50 ng of L-ascorbic acid in 20  $\mu$ l. Spacer, 127  $\mu$ m.

does increase the detector response; Fig. 2 shows that a linear relationship exists between  $\sqrt{u}$  and the detector response. Unfortunately, as predicted by the Van Deemter equation, the effective plate number decreases with increasing flow-rate (Fig. 3).

By using another spacer in the thin-layer cell, it is possible to change the linear fluid velocity in the detector without affecting the flow-rate through the column. Spacers of thickness 51 and 127  $\mu\text{m}$  were used. The increase in  $\sqrt{U_{\text{max}}}$  on using the 51- $\mu\text{m}$  instead of the 127- $\mu\text{m}$  spacer is a factor of 1.5. According to eqn. 6 the detector response also increases by this factor. Fig. 4 shows an increase of a factor 1.3 in the slope of the calibration graph of the detector when the 51- $\mu\text{m}$  spacer is used instead of the 127- $\mu\text{m}$  spacer. This is in reasonable agreement with the predicted factor. Unfortunately, the noise level also increases with decreasing spacer thickness (Fig. 5). The signal-to-noise ratio did not change much, so the spacer thickness hardly influenced the lower detection limit of the detector. Another effect of changing the spacer thickness is an increase in the impedance between the working electrode and the

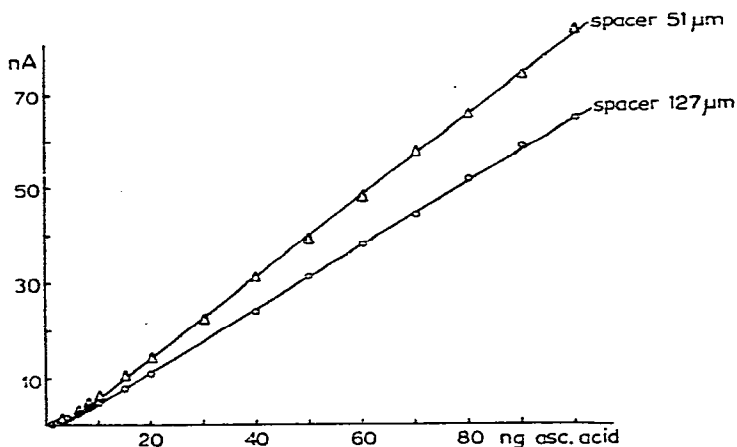


Fig. 4. Effect of spacer thickness on detector response. Column,  $340 \times 2.1$  mm I.D. Nucleosil SB-10 anion exchanger. Eluent, 0.1 M acetic acid buffer (pH 4.5). Potential of working electrodes, 750 mV vs. S.C.E. Flow-rate,  $0.9 \text{ ml} \cdot \text{min}^{-1}$  with the 51- $\mu\text{m}$  spacer and  $1.0 \text{ ml} \cdot \text{min}^{-1}$  with the 127- $\mu\text{m}$  spacer.

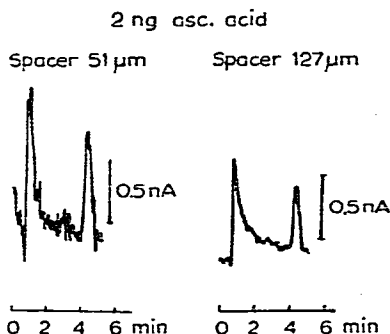


Fig. 5. Effect of spacer thickness on the detector response. Column,  $340 \times 2.1$  mm I.D. Nucleosil SB-10 anion exchanger. Eluent, 0.1 M acetic acid buffer (pH 4.5). Potential of working electrodes, 750 mV vs. S.C.E. Flow-rate,  $0.9 \text{ ml} \cdot \text{min}^{-1}$  with the 51- $\mu\text{m}$  spacer and  $1.0 \text{ ml} \cdot \text{min}^{-1}$  with the 127- $\mu\text{m}$  spacer.

reference and auxiliary electrodes with decreasing spacer thickness (Table I). This can cause deviations in the linear response of the detector at higher concentrations, especially when the aqueous mobile phase is mixed with an organic solvent<sup>1</sup>.

TABLE I  
IMPEDANCE MEASUREMENTS BETWEEN THE ELECTRODES

Electrodes	Impedance ( $k\Omega$ )	
	127- $\mu\text{m}$ spacer	51- $\mu\text{m}$ spacer
Reference electrode-working electrode	20	31
Auxiliary electrode-working electrode	21	32
Auxiliary electrode-reference electrode	1.1	1.4
Working electrode-working electrode	39	63

#### Linear range and detection limits

The detector response is a linear function of the sample concentration, as predicted by eqn. 6. Calculated by the linear least-squares method, the correlation coefficient of the calibration graph in Fig. 6 is  $r^2 = 0.9998$ . The upper detection limit is determined by the maximum detector response of 1000 nA full-scale. The detection limits with a 127- $\mu\text{m}$  spacer in the thin-layer detector cell for 20- $\mu\text{l}$  samples of L-ascorbic acid are given in Table II for columns of different dimensions. Fig. 7 shows the peak of 1 ng of L-ascorbic acid in a 20- $\mu\text{l}$  sample.

It is noteworthy that the linear range of the detector is extended to both higher and lower detection limits compared with the detection limits of the detector as reported previously<sup>1</sup> in flow injection analysis. As a result of dilution of the sample

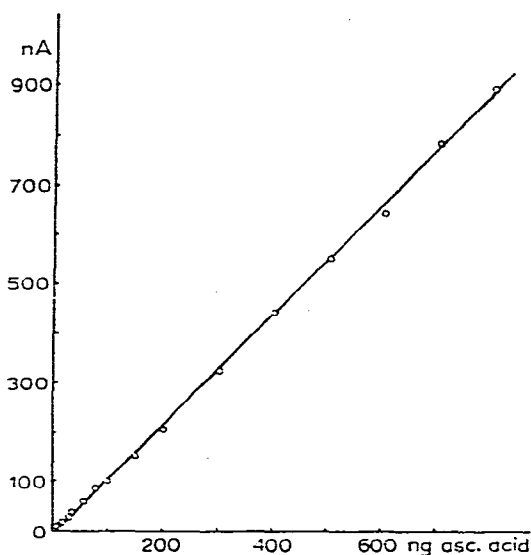


Fig. 6. Graph of the peak height (nA) of the detector response to amount of L-ascorbic acid in 20- $\mu\text{l}$  samples. Column, 250  $\times$  2.1 mm I.D. Nucleosil SB-10 anion exchanger. Eluent, 0.1 M acetic acid buffer (pH 4.5). Flow-rate, 0.8 ml  $\cdot$  min<sup>-1</sup>. Potential of working electrodes, 750 mV vs. S.C.E. Spacer, 127  $\mu\text{m}$ .

TABLE II

## DETECTION LIMITS WITH ANION-EXCHANGE COLUMNS OF DIFFERENT DIMENSIONS

Dimensions of column (mm)	Upper detection limit (ng of L-ascorbic acid per 20- $\mu$ l sample)	Lower detection limit (ng of L-ascorbic acid per 20- $\mu$ l sample)	Correlation coefficient ( $r^2$ ) of calibration graph
150 $\times$ 4.6	1800	1	0.9996
250 $\times$ 2.1	800	<0.5	0.9998

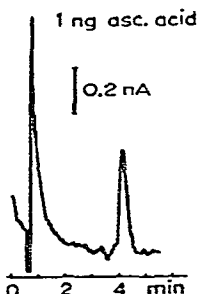


Fig. 7. Detector response for a sample of 1 ng of L-ascorbic acid in 20  $\mu$ l. Column, 250  $\times$  2.1 mm I.D. Nucleosil SB-10 anion exchanger. Eluent, 0.1 M acetic acid buffer (pH 4.5). Flow-rate, 0.8 ml  $\cdot$  min $^{-1}$ . Potential of working electrodes, 750 mV vs. S.C.E. Spacer, 127  $\mu$ m.

through the column it is evident that the upper detection limit will be extended to higher concentrations. In spite of the dilution in the column, the lower detection limit is also lower than without using a column; this is due to the fact that with a column much better pulse damping is obtained. The lower detection limit is no longer limited by pulsations in the flow caused by the reciprocating pump.

*Response of the differential amperometric detector compared with that of a UV detector*

Recently, a spectral study was made of ascorbic acid in buffer solutions of different pH<sup>5</sup>. The isosbestic point of the unionized and the ionized forms occurs at 250.7 nm; the molar absorptivity at this wavelength is 8250 l  $\cdot$  mole $^{-1}$   $\cdot$  cm $^{-1}$ . At pH 4.5 the absorbance at 254 nm is about 83% of the maximum absorbance at 265 nm (the molar absorptivity at 265 nm is 11200 l  $\cdot$  mole $^{-1}$   $\cdot$  cm $^{-1}$ ). Majors<sup>6</sup> has also reported that it is possible to monitor ascorbic acid by liquid chromatography with UV detection. L-Ascorbic acid was therefore chosen as the test compound in this experiment.

In order to obtain a good comparison between the responses of the UV detector and the electrochemical detector, both detectors were connected simultaneously to the chromatograph. The eluent from the column passed first to the UV detector and then to the differential amperometric detector. The responses of both detectors were recorded with a two-pen recorder. No peak broadening in the peaks from the electrochemical detector caused by the UV detector was observed. Fig. 8 shows the correlation between the responses of the UV detector and the differential amperometric detector for samples of ascorbic acid varying from 6 to 100 ng. A correlation coefficient of  $r^2 = 0.9995$  was calculated by the linear least-squares method. The lower

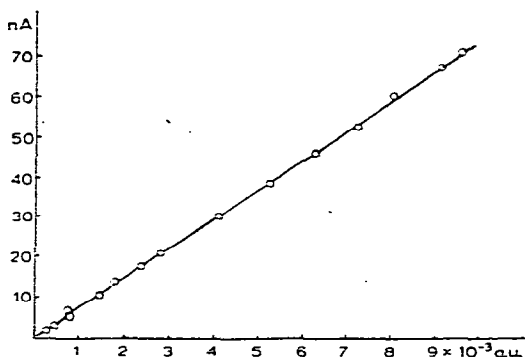


Fig. 8. Correlation between the response of the UV detector and the differential amperometric detector (correlation coefficient  $r^2 = 0.9995$ ). Column,  $340 \times 2.1$  mm I.D. Nucleosil SB-10 anion exchanger. Eluent,  $0.1 M$  acetic acid buffer (pH 4.5). Flow-rate,  $0.8 \text{ ml} \cdot \text{min}^{-1}$ . Spacer,  $51 \mu\text{m}$ . Potential of working electrodes,  $750 \text{ mV vs. S.C.E.}$  Samples,  $6\text{--}100 \text{ ng}$  of L-ascorbic acid in  $20 \mu\text{l}$ .

detection limits of the detectors are  $5 \text{ ng}$  of ascorbic acid per sample for the UV detector and less than  $1 \text{ ng}$  of ascorbic acid per sample for the differential amperometric detector (Figs. 9 and 10).

#### *Determination of ascorbic acid in a pharmaceutical preparation and urine*

**Tablets.** Twenty tablets were accurately weighed and then pulverized to a fine powder. The vitamin C content was determined by anion-exchange chromatography with the differential amperometric detector and by titration according to the British Pharmacopoeia<sup>7</sup>. The assay solution used for the HPLC analysis of the powder was prepared in the following manner.

A  $215\text{-mg}$  amount of powder, accurately weighed, was suspended in  $0.1 N$

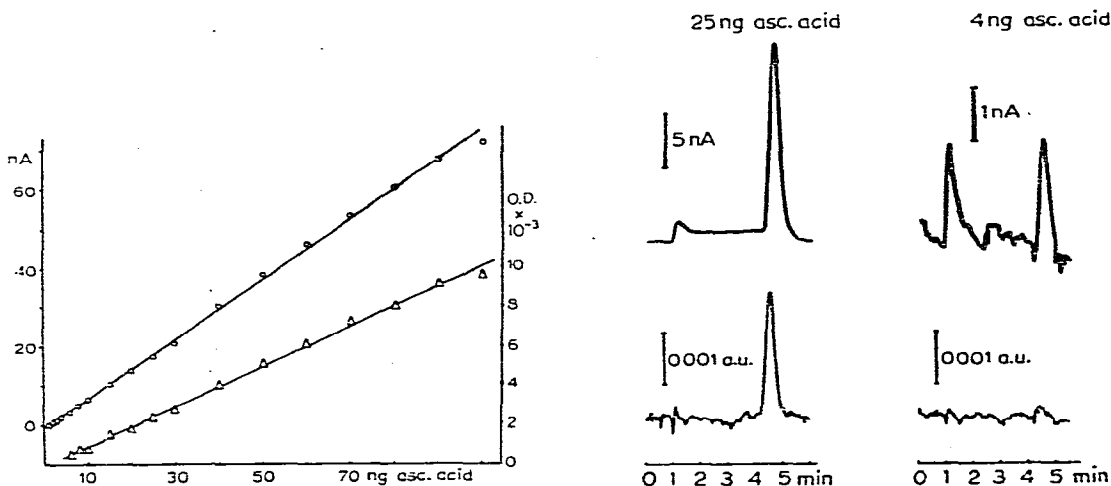


Fig. 9. Calibration graphs for L-ascorbic acid obtained with the UV and the differential amperometric detector. Experimental conditions as in Fig. 7.

Fig. 10. Typical response peaks of the UV and the differential amperometric detector for samples of L-ascorbic acid. Experimental conditions as in Fig. 7.



hydrochloric acid in a 50-ml volumetric flask. About 20 ml of the suspension obtained were transferred into a glass centrifuge tube and centrifuged at 6000 g for 7 min. A 125- $\mu$ l volume of the clear supernatant was pipetted into a 25-ml volumetric flask and diluted with mobile phase (0.1 M acetic acid buffer, pH 4.5).

The ascorbic acid concentration was measured in triplicate by injecting three times a sample of 20  $\mu$ l on to the HPLC column (a 150  $\times$  4.6 mm column of Nucleosil SB-10). The average tablet content was calculated with the aid of a calibration graph.

According to the manufacturer, the average content of ascorbic acid in a tablet is 50 mg. The result obtained by HPLC analysis was 51.9 mg (standard deviation 1.8 mg) of ascorbic acid per tablet (six determinations in triplicate) and by titration 49.2 mg (standard deviation 0.3 mg) per tablet (five titrations). Both results are within 90–110% of the stated amount of ascorbic acid as specified in the USP XIX<sup>6</sup>, and also within 95–107.5% of the stated amount of ascorbic acid according to the British Pharmacopoeia<sup>7</sup>.

It was necessary to make more manipulations in the HPLC analysis than in the titration because of the high sensitivity of the detector, which resulted in a higher standard deviation for the HPLC analysis. However, apart from inaccuracies caused by the sample preparation, the mean standard deviation in the triplicate HPLC determinations was only 0.7 mg, which does not differ significantly from the standard deviation in the titration method (*F* test, *P* = 0.05).

*Urine.* In order to separate the ascorbic acid peak from the other peaks in the chromatograms of urine samples, the acetic acid buffer concentration in the eluent was changed to 0.05 M and the pH was adjusted to 5.0 instead of 4.5. The urine samples were diluted with cold deaerated mobile phase (1:5) and injected directly on to the column. The ascorbic acid peak in the chromatogram was identified by its retention time as measured on a standard solution of ascorbic acid, by addition of an ascorbic acid standard to the urine sample and by spiking an ascorbic acid-free urine sample with ascorbic acid. Ascorbic acid-free urine was prepared by bubbling air through a fresh urine sample at physiological pH for 1 h, followed by deaeration by passing nitrogen through the solution for 2 h. Fig. 11 shows the chromatograms of an ascorbic acid-free urine sample and of an ascorbic acid-free urine sample spiked with ascorbic acid.

In this paper, no concentration levels of ascorbic acid in urine are given, as in this application we wish only to indicate the usefulness of the detector in the analysis in biological fluids.

#### *Stability of the column*

It was difficult to obtain a useful and stable anion-exchange column. The stationary phase [totally porous 10- $\mu$ m silica particles with chemically bonded ion-exchange groups, Si-C bonds and the functional group  $-N^+-(CH_3)_3Cl^-$ ] disintegrated. The disintegration products, which cannot be detected by the UV detector, are electrochemically active and cause background currents which are not compensated for by the reference cell of the detector. Especially when HPLC is started, it takes a few hours to elute all of the disintegration product out of the column. It was found that it was not possible to use the columns for longer than 2–3 weeks because the HETP continuously increased.

The disintegration phenomena are independent of the technique of column

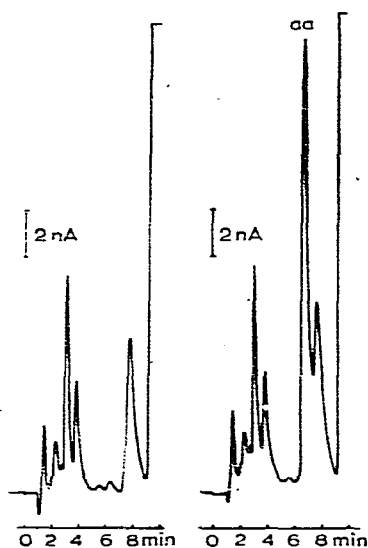


Fig. 11. Chromatograms of an ascorbic acid-free urine sample (left) and of an ascorbic acid-free urine sample spiked with ascorbic acid ( $1.25 \mu\text{g/ml}$ ) (right). Column,  $150 \times 4.6 \text{ mm}$  I.D. Nucleosil SB-10 anion exchanger. Eluent,  $0.05 \text{ M}$  acetic acid buffer (pH 5.0). Flow-rate,  $1.27 \text{ ml}\cdot\text{min}^{-1}$ . Potential of working electrodes,  $750 \text{ mV}$  vs. S.C.E. Spacer,  $127 \mu\text{m}$ .

packing. The columns were packed with a balanced slurry of tetrabromoethane-*n*-butanol, a balanced slurry of carbon tetrachloride, a slurry of carbon tetrachloride with 10% methanol and non-balanced slurries of mobile phase.

Nevertheless, it proved to be possible to determine nanogram amounts of ascorbic acid in urine and in pharmaceutical preparations.

#### ACKNOWLEDGEMENTS

We thank Mr. J. F. C. Nienhuis of the instrumental workshop of our laboratory for constructing the thin-layer flow cell, Mr. A. P. Soesman of the electronic workshop for his assistance in designing the electronics of the detector, Professor Dr. D. A. Doornbos for valuable discussions and his critical reading of the manuscript and Miss M. Kapteyn for typing the manuscript.

#### SYMBOLS

- Re* Reynolds number.  
 $\bar{u}$  Average linear fluid velocity over the cross-section of the flow channel.  
*d* Diameter of flow channel.  
 $d_h$  Hydraulic diameter of the flow channel.  
*A* Cross-section of the flow channel.  
*B* Wetted perimeter of the flow channel.  
*l* Length of the plate.  
*b* Width of the plate.  
*h* Gap between the two parallel plates in the thin-layer cell.

$\delta$	Thickness of the diffusion layer.
$\nu$	Kinematic viscosity.
$D$	Diffusion coefficient of the electroactive component in the solution.
$x$	Coordinate in the direction of flow.
$y$	Coordinate along the normal to the plate.
$U$	Linear fluid velocity far from the plate.
$c_0$	Concentration of the electroactive component in the bulk of the solution.
$j$	Diffusional flux to the plate.
$j_{\max.}$	Maximal diffusional flux to the plate.
$I_{\max.}$	Total diffusional flow to the plate.
$U_{\max.}$	Maximal linear velocity in the parabolic velocity distribution of a plane Poiseuille flow.
$n$	Number of electrons involved in the electrode reaction.
$F$	Faraday constant.

## REFERENCES

- 1 K. Brunt and C. H. P. Bruins, *J. Chromatogr.*, 161 (1978) 310.
- 2 J. A. McGeough, *Principles of Electrochemical Machining*, Chapman and Hall, London, 1974, Ch. II.
- 3 V. G. Levich, *Physicochemical Hydrodynamics*, Prentice-Hall, New York, 1962, Ch. II and XII.
- 4 J. Lankelma and H. Poppe, *J. Chromatogr.*, 125 (1976) 375.
- 5 M. I. Karayannes, D. N. Samios and Ch. P. Gousetis, *Anal. Chim. Acta*, 93 (1977) 275.
- 6 R. E. Majors, *Amer. Lab.*, Oct. (1975) 13.
- 7 *British Pharmacopoeia 1973*, University Printing House, Cambridge, 1973, p. 36.
- 8 *United States Pharmacopoeia*, United States Pharmacopoeial Convention, Rockville, XIX Revision, 1975, p. 37.